Environmental Pollution 229 (2017) 496–504

Contents lists available at ScienceDirect

Environmental Pollution

journal homepage: www.elsevier.com/locate/envpol

Urban emissions hotspots: Quantifying vehicle congestion and air pollution using mobile phone GPS data[☆]

Conor K. Gately [a, b, *], Lucy R. Hutyra [a], Scott Peterson [c], Ian Sue Wing [a]

[a] Boston University, Department of Earth and Environment, 685 Commonwealth Avenue, Boston, MA, 02215, United States
[b] Harvard University, Earth and Planetary Sciences Department, 20 Oxford Street, Cambridge, MA, 02138, United States
[c] Central Transportation Planning Staff, Boston Metropolitan Planning Organization, 10 Park Plaza, Boston, MA, 02116, United States

ARTICLE INFO

Article history:
Received 2 February 2017
Received in revised form
12 May 2017
Accepted 30 May 2017

Keywords:
Emissions
Air quality
Urban
Traffic congestion
GPS
Mobile phone
Inventory

ABSTRACT

On-road emissions vary widely on time scales as short as minutes and length scales as short as tens of meters. Detailed data on emissions at these scales are a prerequisite to accurately quantifying ambient pollution concentrations and identifying hotspots of human exposure within urban areas. We construct a highly resolved inventory of hourly fluxes of CO, NO_2, NO_x, $PM_{2.5}$ and CO_2 from road vehicles on 280,000 road segments in eastern Massachusetts for the year 2012. Our inventory integrates a large database of hourly vehicle speeds derived from mobile phone and vehicle GPS data with multiple regional datasets of vehicle flows, fleet characteristics, and local meteorology. We quantify the 'excess' emissions from traffic congestion, finding modest congestion enhancement (3–6%) at regional scales, but hundreds of local hotspots with highly elevated annual emissions (up to 75% for individual roadways in key corridors). Congestion-driven reductions in vehicle fuel economy necessitated 'excess' consumption of 113 million gallons of motor fuel, worth ~ $415M, but this accounted for only 3.5% of the total fuel consumed in Massachusetts, as over 80% of vehicle travel occurs in uncongested conditions. Across our study domain, emissions are highly spatially concentrated, with 70% of pollution originating from only 10% of the roads. The 2011 EPA National Emissions Inventory (NEI) understates our aggregate emissions of NO_x, $PM_{2.5}$, and CO_2 by 46%, 38%, and 18%, respectively. However, CO emissions agree within 5% for the two inventories, suggesting that the large biases in NO_x and $PM_{2.5}$ emissions arise from differences in estimates of diesel vehicle activity. By providing fine-scale information on local emission hotspots and regional emissions patterns, our inventory framework supports targeted traffic interventions, transparent benchmarking, and improvements in overall urban air quality.

1. Introduction

Poor air quality is a major global problem, with outdoor air pollution causing more than 3.3 million annual premature deaths and many more associated cases of illness (Lelieveld et al., 2015). Mobile sources are responsible for a large fraction of air pollutant emissions in the United States. In 2012, more than 75% of carbon monoxide (CO), and 60% of nitrogen oxides (NO_x) were emitted from on- and off-road vehicles (EPA, 2011a), while mobile sources in large urban areas accounted for as much as 90% of local CO emissions (EPA, 2011b).

Variability in vehicle activity, local meteorology, and urban structure make human exposure to air pollution highly heterogeneous in space and time. More than 45 million people, 14% of the U.S. population, live within 300 feet of a major road, where ambient pollution concentrations from mobile sources are highest and the negative health impacts of exposure to fine particulates ($PM_{2.5}$), CO, and NO_x are most severe (EPA, 2014a). Spatial gradients of concentration and exposure differ by pollutant. For example, concentrations of black carbon (BC) and NO_2 decline sharply on scales of tens to hundreds of meters (Zhou and Levy, 2007; Zhu et al., 2002), whereas CO and $PM_{2.5}$ concentrations can persist for much greater distances from the source (Zwack et al., 2011a). Moreover, in urban areas large buildings surrounding roadways can form 'street canyons' in which vehicular emissions are not rapidly dispersed by atmospheric mixing, causing ambient pollution concentrations to significantly exceed background levels (Zwack et al., 2011b).

☆ This paper has been recommended for acceptance by David Carpenter.

* Corresponding author. Boston University, Department of Earth and Environment, 685 Commonwealth Avenue, Boston, MA, 02215, United States.
E-mail address: cgately@seas.harvard.edu (C.K. Gately).

http://dx.doi.org/10.1016/j.envpol.2017.05.091
0269-7491/

By contrast, estimates of the pollutants emitted by vehicles tend to be constructed at highly aggregated scales, both in space (traffic analysis zones (TAZs) or counties), and/or in time (based on annual fuel sales and consumption (Dallmann and Harley, 2010; McDonald et al., 2012), or on estimates of annual vehicle miles travelled combined with average emissions factors (Harley et al., 2001; Schifter et al., 2005; Zheng et al., 2009)). A key shortcoming of such approaches is that per-kilometer vehicle emissions depend on three classes of variables that are often poorly characterized at fine spatial and temporal scales: vehicle demographics (the shares of car versus truck traffic, fuel characteristics, and the vintages of vehicles' fuel economies and pollution controls), traffic congestion (which affects vehicles' drive-cycles and speed/acceleration profiles) and ambient weather conditions (which affects the performance of engine combustion and emission control devices) (Parrish, 2006). Without such detailed data, generalized spatial proxies (e.g., population, road density) are often used to downscale aggregate emissions estimates (Huang et al., 2011; Olivier et al., 2005), ignoring systematic variations in the local distributions of vehicle types and activity. Although recent advances have demonstrated the feasibility of constructing fine-scale vehicle emission flux estimates without extensive downscaling (Gately et al., 2015; McDonald et al., 2014), comprehensive roadway-level emissions inventories based on actual vehicle activity and fleet composition (e.g. Nyhan et al., 2016) remain rare. The principal difficulties are the lack of direct fine-scale observations, and the consequent need to combine potentially incommensurate datasets to approximate the variability of on-road emissions at sub-kilometer, sub-daily scales. Since vehicle emissions factors are so sensitive to changes in the speed and acceleration profiles of each vehicle (i.e. the 'drive-cycle'), capturing this variability at the relevant time scales (minutes to hours) can significantly improve the accuracy of emissions estimates (Nyhan et al., 2016).

In this paper we demonstrate a novel approach to quantifying emission fluxes at length scales of individual roadway segments and time scales of hours. Air quality models run for urban areas often rely on an emissions inventory generated by a travel demand model (TDM) which uses land use and travel survey data to estimate vehicle trips across an urban domain for an average weekday or weekend day (Lazaridis et al., 2008; Snyder et al., 2014). Emissions factors are then assigned to these vehicle trips to produce daily emissions estimates for different pollutants. Typically, the time resolution of these models is several multi-hour periods, such as the morning and evening peak 'rush-hour' congestion periods, while the spatial resolution is traffic analysis zones (TAZs) that vary in size depending on the model used, but often encompass areas roughly similar to U.S. Census Block Groups (10–20 ha in the denser urban core, 5–10 km^2 in the less dense suburban and rural areas). Here we demonstrate how the traditional TDM approach can be considerably improved upon by leveraging detailed road-specific data on hourly vehicle travel speeds obtained from GPS mobile phone data and hourly traffic volumes from in-road sensors to quantify hourly emissions at the road-scale. Our method combines existing TDM estimates of vehicle trips with additional individual pieces of information over the large urban domain of Eastern Massachusetts, assimilating data at various native spatial and temporal resolutions into a consistent framework. The resulting high-resolution emissions inventory is then used to quantify the relative contributions of hotspots and congestion to urban air quality, and to test the local fidelity of existing coarse-scale inventory products.

2. Methodology

The focus of the present study is the 8640 km^2 metropolitan area surrounding Boston, Massachusetts, which encompasses the 101 towns that make up the Boston Metropolitan Planning Organization (MPO) jurisdiction and includes a broad range of road types, settlement patterns and traffic congestion levels (Fig. 1). This area regularly ranks in the top 5 of U.S. urban areas for traffic congestion (Schrank et al., 2012) and the top ten for total vehicle miles traveled per year (FHWA, 2012a). GPS data from in-vehicle mobile phones and on-board navigation systems were used to quantify hourly vehicle speeds on over 67,000 road segments across the domain. We paired vehicle speed data with hourly traffic volume data obtained from in-road sensors to model hourly vehicle activity across the entire regional road network for the year 2012. We calculate emissions for each hour of the year (indexed by h), estimating the flux of five pollutants (CO, NO_2, NO_x, $PM_{2.5}$ and CO_2, indexed by p) emitted by vehicles on each of 280,424 road segments (indexed by l). Pollutant species are emitted by v types of vehicles, traveling at speeds that we discretize into s 5-mph intervals. Each road segment's hourly emission flux ($\mathbf{q}^*$) is the product of the vehicle kilometers traveled (VKT, $\mathbf{k}^*$) on it and an emission factor ($\mathbf{f}^*$) for every combination of v and s, defined as a response surface that is a function of spatially and temporally varying temperature ($\mathbf{T}$) and relative humidity ($\mathbf{H}$):

$$\mathbf{q}^*_{p,l,h} = \Sigma_v \Sigma_s \mathbf{k}^*_{v,s,l,h} \times \mathbf{f}^*_{p,v,s}\left[\mathbf{T}_{l,h}, \mathbf{H}_{l,h}\right] \quad (1)$$

We construct a suite of emission factors to encompass the range of vehicle types, travel speeds, and meteorological conditions observed in our study domain from multiple customized runs of the EPA Motor Vehicle Emissions Simulator (MOVES) version 2014a, (EPA, 2014b) with key inputs—county-specific data on fuel composition, vehicle fleet age and composition, and historical meteorology—customized with local data from our domain and target year. Our meteorological variables were obtained from the North American Land Data Assimilation System (NLDAS-2), which reports 0.125° gridded hourly temperature and specific humidity (Xia et al., 2012). Vehicle fleet age distributions and fuel formulation distributions were provided by the Boston MPO. Output from MOVES included combined emissions factors (for running and evaporative emissions) for each pollutant, stratified by vehicle type, road type, fuel type, vehicle speed, ambient air temperature, and relative humidity.

Our fundamental methodological advance is the linking of emission factors to imputed flows of different types of vehicles on a particular road segment in a given hour and traffic speed interval. For this we utilize a high-resolution database of directly measured vehicle speeds obtained from mobile phone and on-board vehicle navigation GPS data provided by the traffic consultancy firm INRIX. The raw data record vehicle speeds on more than 67,000 individual road segments in the study area at 5-min intervals. For computational tractability, these observations were aggregated to produce hourly mean speeds, which were matched to road segments.

The INRIX data over-represent large- and medium-sized roads, which although they account for only 15% of the total road length in kilometers across the domain, represent more than 70% of the total annual VKT. On the road segments for which there were no INRIX records, we imputed speeds based on volume-delay functions (VDF) that relate hourly traffic volumes to average traffic speed using the capacity of the road segment and its typical 'free-flow' speed (Dowling, 1997). VDF parameterizations were taken from the TDM, which uses a modified Bureau of Public Roads (BPR) formula that varies by road functional class and rural-urban context (Eqn. S(1) in the Supporting Information). Because unmodified BPR-based VDFs have been shown to overestimate speeds in congested conditions, the formulas used by the TDM have been calibrated using local traffic counts and directly measured speeds using

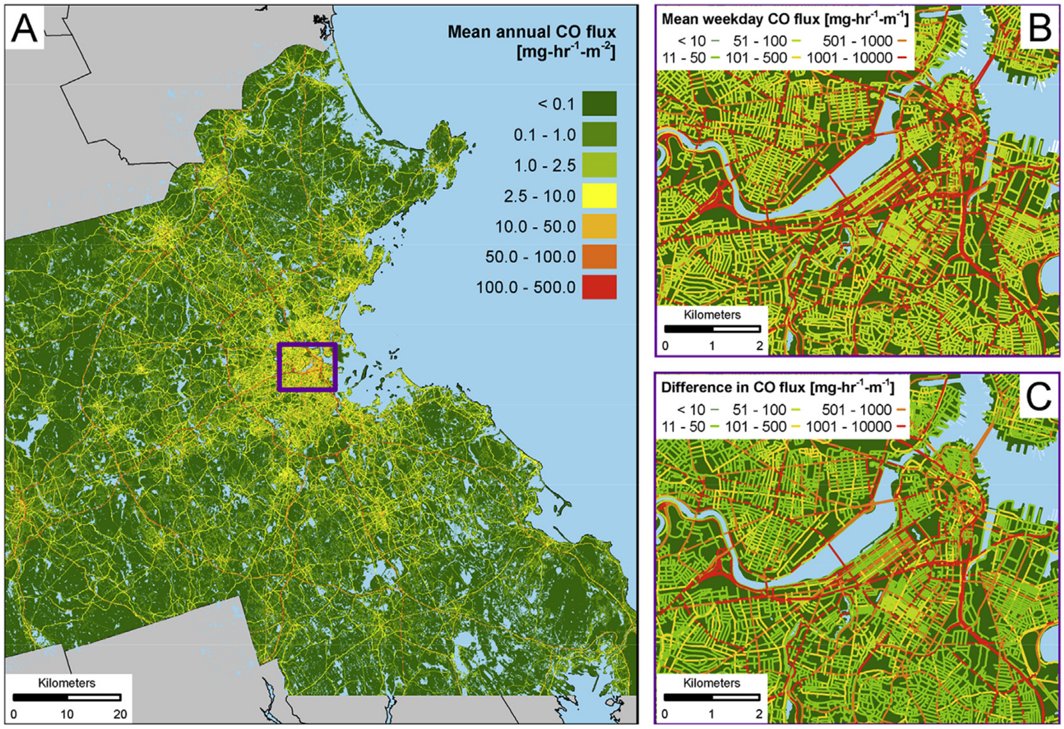

Fig. 1. Annual mean hourly CO flux for study domain (Panel A). Panels B and C show a 65 km^2 area surrounding downtown Boston described by the purple box in Panel A. The mean hourly CO flux during weekday evening peak periods (3pm–7pm) is shown in Panel B, while Panel C shows the difference between the weekday evening CO flux and the overall mean weekday flux (same color scale). Freeway and major arterial emissions are 25–50% higher during evening peak compared to mean daytime emissions. (For interpretation of the references to colour in this figure legend, the reader is referred to the web version of this article.)

'floating car' data across a wide range of traffic conditions. However, this method results in only 4% of non-INRIX road segments being classified as experiencing significant congestion, mostly in the core of the urban area surrounding downtown Boston. We consider this to be a conservative estimate, because of the challenges of accurately modeling low vehicle speeds under heavy congestion (Dowling, 1997; Dowling and Skabardonis, 1993; Skabardonis and Dowling, 1997). To identify whether traffic flow by link and hour falls into a given speed bin we use the indicator variable $\delta_{s,l,h}$.

Our estimates of vehicle activity were constructed by integrating vehicle volumes estimated by vehicle type for each road segment in the TDM with traffic counts derived from the Massachusetts Department of Transportation (MDOT) road sensor network. Boston MPO's TDM is a traditional four-step model run in the TransCAD transportation planning software (Boston MPO, 2017). The model uses as inputs data on local land-use, demographics, zoning, and a 2010 statewide travel survey (Massachusetts DOT, 2012) to generate estimates of trip origins and destinations for personal and freight transportation across the study domain. Trips are assigned to multiple modes of travel, including vehicles, carpooling, public transit, cycling, and walking. The model then assigns vehicle trips, stratified by vehicle class (passenger cars, passenger trucks and SUVs, medium-duty trucks, and heavy-duty trucks and buses) to the road network using optimization algorithms that account for road capacity and levels of congestion. Traffic volumes by vehicle type on each road segment (separately for each direction, in the case of two-way roads) are calculated at four time periods of an average weekday, given by the index t—AM peak (6am–10am), Mid-Day (10am–3pm), PM peak (3pm–7pm), and Night (7pm–6am). The resulting model output, which we denote $G_{v,l,t}$, lacks the temporal resolution needed for hourly emissions estimates. We therefore utilize it to determine the distribution of vehicle types on a given road segment during the hours within each aggregated TDM time period. To this end we calculated each vehicle class' share of the total volume on each road segment in each period, denoted as $\chi_{v,l,t}$:

$$\chi_{v,l,t} = \frac{G_{v,l,t}}{\Sigma_v G_{v,l,t}} \tag{2}$$

We obtain traffic data from two sources: estimates of average daily traffic volumes (ADT) for every road in the study domain from MDOT's annual Massachusetts Road Inventory (A_l), and hourly traffic counts on 62 major and minor roads in the study domain from MDOT permanent traffic recorders ($k_{l',h}$). From the latter data we derived hourly allocation factors that we used to partition the former annual link volumes (ADT x 366 days) among every hour of 2012. To overcome the sparsity of traffic count data, allocation factors were assigned to road segments using a nearest-neighbor algorithm

$$\alpha_{l,h} = \frac{k_{l',h}}{\Sigma_{h'} k_{l',h'}} \quad if\ l \in \mathcal{N}\left(l'\right) \tag{3}$$

where $\mathcal{N}(l')$ denotes the spatial neighborhood surrounding each traffic recorder. The resulting imputed hourly traffic volumes were then further divided among different vehicle types using the TDM's outputs for the corresponding road link and intra-day time-step, and all vehicles were assigned the speed of the traffic on that link at that hour

$$\mathbf{k}^*_{v,s,l,h} = \psi_{v,h} \times \delta_{s,l,h} \times \alpha_{l,h} \times A_l \times \chi_{v,l,t} \quad if\ h \in t \tag{4}$$

MDOT vehicle classification counts indicated that weekend truck activity was on average 25–35% of weekday levels, so truck volumes during weekend hours were scaled downward by the appropriate amount (indicated by the vehicle-hour adjustment factor $\psi_{v,h}$). Our final step was to calculate separately the emissions from passenger vehicle cold starts, using emission factors from MOVES and detailed estimates of household vehicle trips across the domain obtained from the travel survey (Massachusetts DOT, 2012). Details of the methodology are provided in the Supporting Information (SI). Datasets of our emissions estimates are publically available for download at http://dx.doi.org/10.7910/DVN/4YGU5J.

3. Results and discussion

3.1. Regional emissions totals

For the study area in the year 2012 we estimate that running vehicles emitted 134.1 Gg of CO, 2.8 Gg of NO_2, 61.2 Gg of NO_x, 2.4 Gg of $PM_{2.5}$, and 20,734 Gg of CO_2. Additional emissions from passenger vehicle cold engine starts are 72.9 Gg of CO, 5.5 Gg of NO_x, 0.1 Gg of $PM_{2.5}$, and 650.1 Gg of CO_2. At the pixel scale (100 m × 100 m grid cells), the mean annual surface fluxes per unit of land area were 27.2 g-m^{-2} of CO, 8.0 g-m^{-2} of NO_x, 0.3 g-m^{-2} of $PM_{2.5}$, and 2810.9 g-m^{-2} of CO_2. Vehicle starts account for a small fraction of the total emissions of most species (4.8% of $PM_{2.5}$, 8.3% of NO_x, and 3% of CO_2), with the exception of CO (35%). This estimate is conservative, as start-up emissions from non-passenger vehicles could not be reliably estimated. The comparatively large share of CO from cold starts is a function of the large number of trips by passenger cars throughout the study domain, a short average trip distance due to the Boston metro area's high population density, and the region's cool ambient temperatures.

3.2. Air-pollution impacts of traffic congestion

Vehicles' fuel economy and emission rates rise as their average speed declines, due to the increased engine load required for re-acceleration, in conjunction with the power-efficiency curve of internal combustion engines (Figs. S4 and S5) (West et al., 1999; Zhang et al., 2011). A key advantage of the INRIX dataset is that it enabled us to use Eq. (1) to quantify the air pollution burden of reductions in vehicle speed due to road traffic congestion at multiple spatial and temporal scales. We simulate two alternative scenarios to explore the air pollution consequences of moving to congestion-free patterns of traffic and specific emissions: the first is a hypothetical expansion of road network capacity to accommodate current travel with no loss of service, while the second alleviates congestion through volume-reduction measures that are perfectly targeted in time and space.

Scenario (i) increases the speed of baseline traffic flows on every road segment to their respective free-flow velocities throughout 2012. Traffic volumes are maintained at baseline levels: they neither decline to the levels necessary to attain free-flow speed under current road capacity, nor increase because of 'induced demand' incentives for individuals to take advantage of road capacity expansion by driving more (Cervero and Kockelman, 1997; Ewing and Cervero, 2001; Hymel et al., 2010; Noland, 2000; Small and Van Dender, 2007). The results thus indicate the potential emission reductions from eliminating present-day vehicle traffic congestion. Scenario (ii) reduces the traffic volume on each segment at congested hours to the level necessary to attain free-flow speed. For hours where observed speeds were below free-flow speeds, we artificially reduced traffic volumes to the maximum volume that was otherwise observed on the link while speeds were still at free-flow conditions. No adjustments in traffic volumes were made for those hours where observed speeds were at or above free-flow levels. The concomitant VKT reductions are the cost of successfully managing congestion.

Scenario (i) generates region-wide emission reductions that are small, ranging from 3.7% to 6.1% for different pollutants (Table 1). However, on individual roadways pollution abatement from eliminating congestion can be far larger. These benefits tend to occur within the urban core, on downtown Boston's heavily trafficked freeways and arterials (Fig. 2), where emission reductions can be 25%–75% or higher, depending on the pollutant. For pollutants emitted mainly by diesel vehicles (NO_x and $PM_{2.5}$), the relative reductions in emissions from eliminating congestion are larger for $PM_{2.5}$ than for NO_x, reflecting variation in the shapes of different pollutants' emission-speed curves. For example, for heavy trucks there is a notable increase in $PM_{2.5}$ emission rates at speeds of 35mph and below, in contrast to NO_x emissions rates which tend to increase somewhat more smoothly and slowly as speeds decrease (Figs. S4 and S5). We identify multiple areas of particularly high emissions ("hotspots"), the bulk of which are located near freeways, freeway ramps, and major urban arterials. The spatial distribution of these hotspots was highly heterogeneous. Certain corridors and intersections experienced very large amounts of both emissions and congestion, while nearby roads with similar attributes remain uncongested, exhibiting moderate emissions. We also observed large temporal variations in emissions, with weekday morning and evening peak periods having the highest levels for all pollutants. Weekday evening emissions were in many places 25–50% higher than mean daytime emissions (Fig. 1C). Patterns of traffic congestion, as well as the relative contribution of congestion to emissions, were also highly variable in space and time (Fig. 2).

We also found that many of the locations in Boston's urban core that have the highest estimated emissions were distant from the AQS monitoring stations in Kenmore and Dudley Squares (Fig. 2B, white and grey circles, respectively). The 25 ha areas surrounding these stations show very limited contributions from local congestion (Fig. 2E and F). As a contrasting congestion-dominated example, mean daily emissions of NO_x and CO at a location several kilometers west of the stations (Fig. 2B, white square) were found to be between five and eight times higher (Fig. 2G–H) than the emissions levels immediately surrounding the stations (Fig. 2E–F). This result has important implications for the efficacy of traditional emissions monitoring protocols. While CO is a relatively long-lived molecule in the atmosphere (Wang and Prinn, 1999), NO_2/NO_x undergoes significant secondary reactions within hours of being emitted in urban areas (Streets et al., 2013). The sparsity of the AQS network suggests that measured NO_2/NO_x concentrations are unlikely to reflect the high concentrations of these pollutants in emission hotspots several kilometers away. Our identification of the latter locations thus provides insight into future site selection for additional short- and long-term air quality monitoring.

The effects of eliminating congestion vary substantially over the course of the day, with patterns that differ by pollutant and location. For NO_x (Fig. 2E and G), congestion amplifies emissions both during the middle of the day, when truck traffic tends to be highest, and in the late evening. For CO (Fig. 2F and H), congestion enhancement is large and persistent across the entire late afternoon and evening hours. For all pollutants there is pronounced variability in congestion enhancement during the middle of the day, when hour-to-hour fluctuations in average traffic volumes are largest. In general, the locations with the largest congestion-related amplification of emissions are roads and intersections that have both high levels of traffic throughout the day, as well as regular, persistent, heavy congestion (Fig. 2B, G, H).

Scenario (ii) generates noticeably larger—through still comparatively modest—aggregate pollution abatement (7.5%–9.5%), at the cost of a 4.1% reduction in annual region-wide VKT. The fact that emission reductions can be more than twice as large as the

Table 1
Annual total emissions for study domain compared to estimated emissions under two mitigation scenarios: (i) Speed Improvement – wherein traffic congestion is eliminated but vehicle volumes remain the same; and (ii) Volume Reduction – wherein vehicle volumes are reduced on congested roads by an amount sufficient for traffic to travel at free flow speeds at all times.

Pollutant	Running emissions [Gg]	Scenario (i) Speed improvement [Gg]	Scenario (ii) VKT reduction [Gg]
CO	134.1	129.0 (−3.8%)	123.6 (−7.8%)
NO_2	2.79	2.69 (−3.7%)	2.58 (−7.5%)
NO_x	61.1	58.8 (−3.8%)	56.5 (−7.6%)
$PM_{2.5}$	2.39	2.25 (−6.1%)	2.16 (−9.5%)
CO_2	20,734.0	19,622.7 (−5.4%)	18,830.3 (−9.2%)

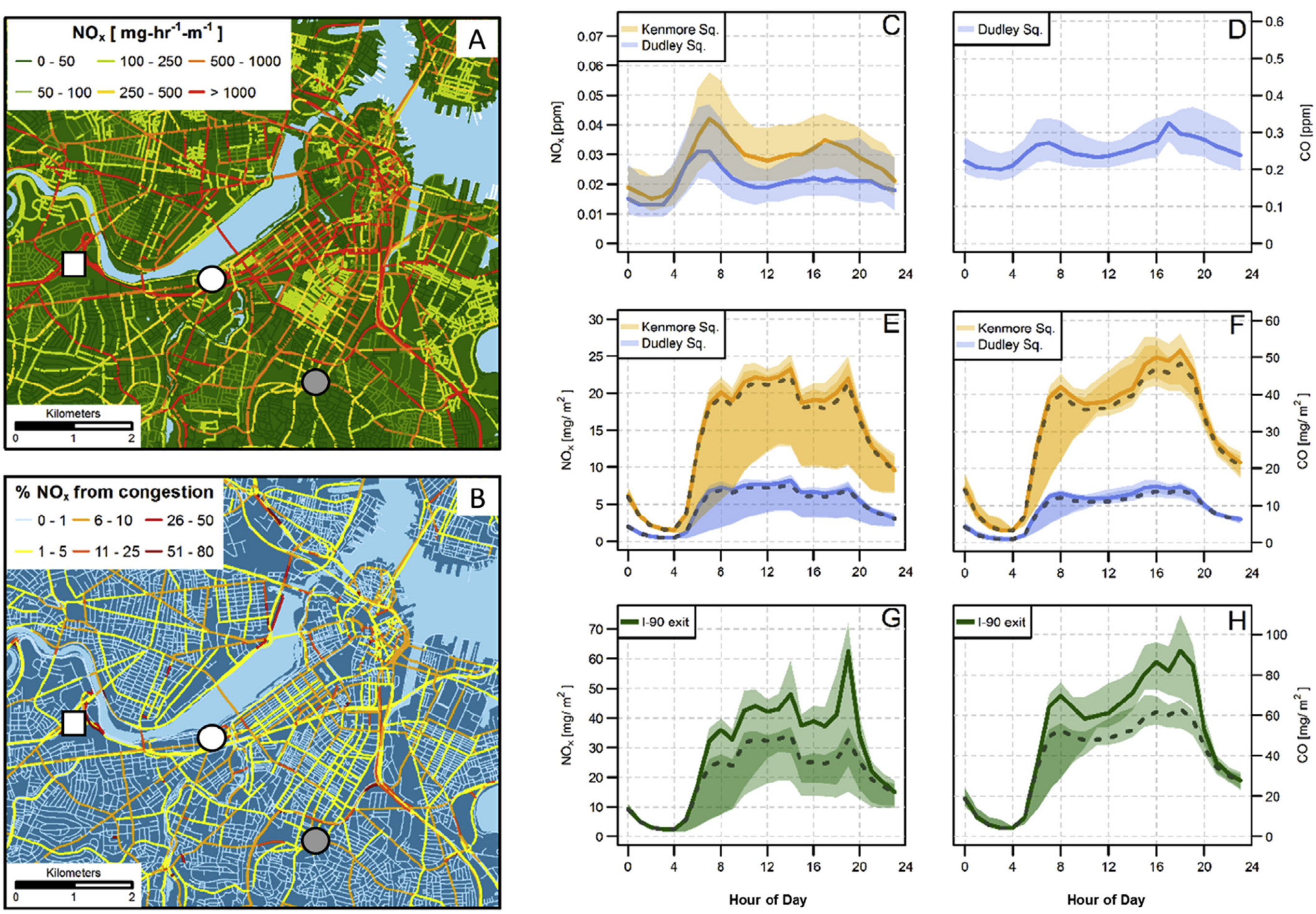

Fig. 2. Panel A shows mean weekday daytime NO_x fluxes in the metro Boston urban core. Panel B shows the percent of total weekday daytime NO_x emissions that occur solely due to congested traffic conditions. Panels C–D show median and interquartile range of ambient NO_x and CO concentrations measured at the EPA AQS stations in Kenmore and Dudley Squares, (white circle and grey circle in panel A, respectively). Panels E–F show median diurnal weekday NO_x and CO fluxes for grid cells within 500 m of the AQS stations. Panels G–H shows equivalent fluxes at an emissions 'hotspot': Interstate-90 near a major exit ramp (white square). Solid lines show 2012 estimates, grey dashed lines show estimated fluxes if traffic congestion was eliminated. Shaded areas represent interquartile ranges of annual hourly emissions/concentrations.

declines in VKT that they require suggests that finely targeted VKT reductions may be attractive as an air quality management strategy, especially for pollutants emitted predominantly by diesel vehicles (NO_x and $PM_{2.5}$). As in the previous scenario, in percentage terms there is the potential for considerable abatement at the local scales where air pollutants exert deleterious impacts on human health.

Less optimistically, our results drive home the simple fact that the vast majority of vehicle air pollutants are emitted during non-congested travel. The main features of the aggregate distribution of vehicle speeds through the domain (Fig. 3A) are that over 87% of VKT occurs under free-flow conditions (ΔMPH < 5), and that most of the congested travel involves only modest speed reductions. The largest increases in per-km emissions rates above their free-flow levels occur when speed reductions are significant (ΔMPH > 20; Fig. 3B), especially for arterial roads with already low free-flow speeds. However, across our domain only 7.1% of total VKT was subject to such heavy congestion, accounting for roughly 11–13% of total regional emissions, depending on the pollutant. Even in the City of Boston, 80% of VKT occurred at speeds at or within 5 miles per hour of free-flow conditions, and only 8% of VKT experienced >15mph speed reductions. These results are consistent with other studies such as Barth and Boriboonsomsin (2008) who found that for roads in Los Angeles, CA, short-term, localized enhancements of CO_2 emissions from congestion could be large (20%–40%), but overall total enhancements remained modest (~7%), due to a distribution of VKT by speed that was similar to the distribution we

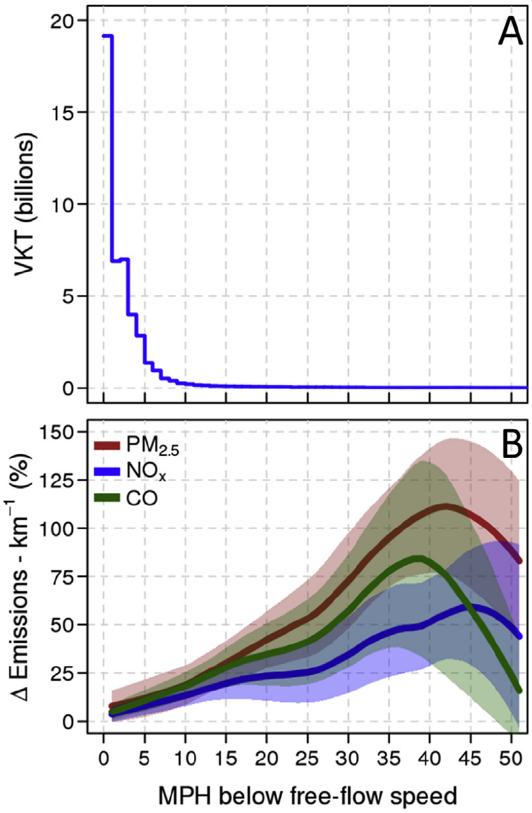

Fig. 3. Distribution of annual VKT by congestion intensity (Panel A). Congestion intensity is expressed as the difference between free-flow and observed speeds. Panel B shows the percent change in emission rates of $PM_{2.5}$, NO_x, and CO as a function of congestion intensity. Over 87% of VKT in the domain is uncongested ($\Delta MPH < 5$), and of the VKT that is congested, over 50% experiences only moderate speed reductions of 5–15 MPH.

observed in our study area (i.e. 80% of VKT occurring at free-flow speeds).

In addition to environmental impacts, it is commonly reported that congestion results in a large amount of 'excess' fuel and money, as vehicles are running at reduced fuel economy when in traffic. For example, the Texas Transportation Institute's Urban Mobility Report (UMR) (Shrank et al., 2012) calculates annual estimates of the amounts of 'excess' fuel, money, and time spent by drivers as a result of traffic congestion for hundreds of urban areas across the United States.

The Boston Urbanized Area often ranks in the top five or top three most congested urban areas in the U.S., according to different metrics calculated in the UMR. Our model output for Scenario (i) indicates that in 2012 traffic congestion across our entire Eastern Massachusetts domain resulted in the consumption of an 'excess' of 80.97 million gallons of gasoline and 32.84 million gallons of diesel fuel. To more directly compare our results to the UMR, we subset our domain to the Boston Census Urbanized Area boundaries (to match the geography used by the UMR). For this sub-domain, our estimate of 'excess' congestion-associated fuel consumption is 61 million gallons, similar to the 70 million gallons reported in the 2012 UMR (Shrank et al., 2012). Using 2012 average prices for gasoline and diesel in Massachusetts ($3.53 per gallon and $3.93 per gallon, respectively) this congestion-derived fuel consumption resulted in $414.9 million in 'excess' fuel expenditures for drivers in our study area. Although not small, this 'excess' fuel use is modest relative to the total fuel consumed, similar to our emission reductions in Scenario (i). In 2012 Massachusetts consumed over 3.2 billion gallons of motor fuel (FHWA, 2012b), making fuel consumption due to traffic congestion equivalent to only 3.5% of the statewide total.

We thus reiterate the relatively minor importance of congestion's impacts on emissions, fuel, and costs at regional or national scales. For policymakers, the main value in congestion mitigation continues to lie in targeting speed improvements for the most severely congested locations to improve both traffic flow and local air quality. Overall, large-scale abatement of vehicular pollution will require significant reductions in road travel and/or substantial improvements in the per-km emissions performance of the vehicle fleet (via enhanced pollution control technologies and/or shifts to electric and other low-emission vehicles).

3.3. Robustness

A key test of the robustness of our emission model framework was the comparison of estimates of CO_2 with the DARTE inventory (Gately et al., 2015) for the same geographic domain. The two estimates were in good agreement (Fig. S2), with 20,734 Gg CO_2 for our new inventory and 22,421 Gg CO_2 for DARTE. This is an encouraging result, as DARTE relies on a much coarser distribution of vehicle types, and employs state-level average fuel economy factors that do not account for the impacts of vehicle speeds and congestion on fuel use. The main difference from DARTE is urban and rural areas' relative contributions to total emissions. On average, DARTE emissions are lower in the urban core and inner suburbs compared to our model, but higher on the large freeways and in the lower density outer suburbs and rural areas. We attribute this disparity to the different data sources that underlie DARTE—especially the traffic counts, which were disaggregated from the county level solely by road functional class. This procedure results in a 'smearing' of emissions across all of the roads of a certain class in each county. By contrast, the current model directly captures the spatial variation in traffic on each functional class of road within each county, as every road segment has a unique value for ADT estimated from local traffic counts.

We also compared our results to annual reported on-road vehicle emissions at the county scale in the 2011 EPA National Emissions Inventory (NEI) (EPA, 2011c). Despite small differences in the domain-wide aggregate annual emissions of CO (<5%), our estimates of several other pollutants diverged from the NEI (Table 2). Relative to the present inventory, average NEI emissions are 18% lower for CO_2, 38% lower for $PM_{2.5}$, and 44% lower for NO_x. This finding contributes additional results to the extensive body of ongoing research aimed at evaluating the accuracy of NO_x emissions inventories across the U.S. Some studies have found that the NEI overestimates mobile source NO_x emissions relative to surface and/or satellite measurements (Anderson et al., 2014; Kim et al., 2016), while others have found that the NEI both over- and underestimates surface measurements depending on the year and the spatial region (Xing et al., 2013). The accuracy of both diesel heavy vehicles' activity levels and emissions factors are key uncertainties, with NO_x emission estimates being most sensitive to these inputs

Table 2
Annual total emissions for the five Massachusetts counties in our study domain compared to emissions estimates from the 2011 EPA National Emissions Inventory (NEI2011v2), and our no-congestion Scenario (i).

Pollutant	EPA NEI 2011v2 [Gg]	This Study [Gg]	Scenario (i) [Gg]
CO	162.72	170.03	167.05
NO_x	3.018	5.538	5.408
$PM_{2.5}$	1.329	2.104	2.008
CO_2	14,523.21	17,397.69	16,213.08

(Koupal et al., 2014).

Given the NEI's agreement with our estimates of CO emissions, which are predominantly due to gasoline vehicle activity (EPA, 2015a), the likely drivers of the discrepancies in $PM_{2.5}$ and NO_x are differences in (a) diesel vehicle VKT, (b) $PM_{2.5}$ and NO_x emission factors, and/or (3) the MOVES drive cycle and vehicle speed profiles relative to INRIX observations. The fact that the NEI's emission factors are obtained from the same version of MOVES used here enables us to rule out (b) as a substantial source of deviation. But the implicit consistency of underlying gasoline vehicle VKT, combined with the 18% difference in the two inventories' CO_2 emissions, suggests that differences in diesel VKT (a) are the likely cause. To evaluate the impact of drive-cycle differences (c), we compared NEI against emissions from our no-congestion Scenario (i), and found that congestion elimination does reduce the discrepancy, but only by 1–3% (Table 2). We find it unlikely that the remaining differences in NO_x and $PM_{2.5}$ emissions can be explained by the difference between the MOVES truck drive-cycle and our 'free-flow' scenario, especially since the MOVES drive cycle attempts to capture the wide variety of traffic conditions that exist on urban roadways (EPA, 2015a). It thus seems that the majority of the divergence is due to aggregate differences in diesel vehicle activity, with minor contributions from differences in vehicle speeds and ambient meteorology.

This line of reasoning is broadly consistent with tests by Koupal et al. (2014) of the relative influence of the different MOVES inputs submitted by states' to the 2011 NEI. Koupal et al. (2014) found that although the median value for the shares of VKT comprised of medium and heavy trucks that were submitted to MOVES was quite similar in magnitude to the default values used by MOVES, the 90th percentile of truck VKT shares was almost double the default value. The upshot of running MOVES at the 90th versus the 10th percentile of state-submitted truck shares was a difference of >50% for total daily NO_x and >100% for total daily $PM_{2.5}$. The large differences between our inventory and the 2011 NEI are thus within the range of variation reported by Koupal et al. (2014), suggesting that relative to the MOVES default values, the truck VKT shares estimated by the TDM for eastern Massachusetts are well within the range of variation observed across all U.S. counties. This assessment underscores the importance of efforts to further improve the accuracy of truck VKT and emission factor data submitted to EPA by the states for the preparation of the NEI.

3.4. Impacts of future climate change

To assess the impact of climate warming on transportation related emissions we adjusted our meteorological inputs using mean monthly temperatures in 2050 under the SRES A2 scenario (IPCC, 2000) reported by the National Center for Atmospheric Research (NCAR) Community Climate System Model (CCSM) (NCAR, 2012). We made no adjustments to the relative humidity values in our base case 2012 meteorology, only adjusting hourly temperatures by the difference between the 2012 NLDAS-2 monthly mean temperatures and the 2050 CCSM forecast monthly mean temperatures. All other model parameters, including vehicle fleet mix and 2012 traffic congestion were held constant. The results capture changes in emissions arising solely from changing temperatures.

Across our domain we find a roughly 2.5% rise in emissions of both CO and NO_x, with many local areas experiencing larger increases. While running emissions rates of CO and NO_x are relatively insensitive to ambient temperature (EPA, 2015b), warming does have an indirect effect on their emissions rates. Higher summer temperatures result in increased usage of vehicle air-conditioning, fuel consumption per kilometer travelled, and by extension overall vehicle emissions (Choi et al., 2010). While the magnitude of this effect is modest, at the regional scale it is on par with the potential emissions reductions achieved in Scenario (i), above. Regardless whether congestion mitigation policies are implemented over the next several decades, the region is likely to experience modest increases in emissions arising solely due to warming temperatures. The upside, albeit modest, is that higher winter temperatures result in slightly lower emissions of $PM_{2.5}$ (0.6%), driven by reductions in the number of starts and hours of vehicle operation under cold temperatures that are associated with poor fuel combustion and high particulate emission rates. The caveat is that the region-wide reduction in $PM_{2.5}$ emissions obscures several areas where local emissions may increase by similar small amounts.

On balance, this mixed picture of warming temperature effects on emissions suggests that the consequences of climate change for regional air quality will be broadly negative, as rising temperatures, particularly in the summer months, are likely to enhance vehicle emissions of the ozone-precursor pollutants CO and NO_x. These estimates do not account for the potential impacts of higher temperatures on vehicle activity and traffic congestion, or the secondary chemistry associated with production of low-level ozone and other respiratory irritants. The latter are anticipated to be yet another harmful consequence of changes in the climate (Jacob and Winner, 2009; Kinney 2008; Steiner et al., 2006).

3.5. Summary and implications

The key advantage of our modeling framework is its ability to bridge the gap between the fine temporal scale and highly localized air quality records from AQS monitors and the annual county-level estimates of pollutant emissions reported by the NEI. Assimilating vehicle speed and volume data based on detailed local model outputs facilitates quantification of pollution emitted by traffic on individual road segments in every hour of the year across a large study domain. Using actual vehicle speeds instead of the default MOVES drive cycle enables us to disentangle the effects of traffic congestion on emissions at both regional and local scales, highlighting the specific locations where mitigating congestion via VKT reductions can yield the largest reductions in emissions of vehicular air pollutants. Our finding of a modest overall impact of traffic congestion on emissions at broad spatial scales is tempered by the finding that congestion significantly enhances emissions in many localized areas within the study domain, revealing a clear potential for significant emissions reductions by targeting mitigation efforts at key hotspots.

The sparsity of in-situ air quality measurements remains a persistent obstacle to explicit modeling of the spatiotemporal patterns in urban air quality, both in the U.S. and in the developing world. Sensor networks such as the AQS provide valuable data for the calibration and validation of regional air quality models, but these simulations cannot fully infer the spatial and temporal structure of atmospheric concentrations using these sparse surface measurements alone (Lauvaux et al., 2012; Wu et al., 2011). Developing countries frequently lack both air quality monitoring and traffic activity data. However, because mobile phone and GPS data are widely available even in developing countries, our methodology offers a potentially fruitful way to improve estimation of vehicle tailpipe emissions, urban air quality and human health impacts in the developing world.

Bottom-up inventories will continue to play a critical role in urban air quality surveillance by establishing the best *a priori* estimate of emissions source activity across a given geographic domain. Especially in urban areas with widely spaced monitors, estimating localized changes in air quality across the large areas between stations remains challenging in the absence of additional data or measurements. Localized variations in atmospheric mixing and secondary chemical reactions can significantly dilute or intensify pollution concentrations over distances as short as a few hundred meters (Zhou and Levy, 2007), limiting the ability of monitor data to capture short-lived, highly localized enhancements in pollution concentrations.

Initiatives such as the C40 Cities Climate Leadership Group internationally and the Compact of Mayors in the United States, have propelled cities to the forefront of efforts to improve air quality. Nevertheless, in order to make genuine progress toward their objectives of reducing emission cities will need transparent, reproducible and easily implementable methodologies to track the pollution emitted by vehicles on an ongoing basis (Hutyra et al., 2014). The approach outlined in this paper has both the granularity necessary to inform local policy interventions that can make meaningful changes in a city's emissions profile at the human-scale (Gurney et al., 2015), and the extensibility to facilitate its implementation in a wide range of urban contexts. This is especially important given recent and upcoming satellite missions (e.g. OCO-2, OCO-3, TROPOMI, TEMPO, GeoCARB) that are poised to provide unprecedented views of both urban CO_2 profiles and broader urban air quality worldwide. Coupling satellite observations with the type of high resolution emissions modeling described here is an important step toward improving our ability to monitor air pollution concentrations in urban areas, target mobile sources emission reductions in space and time, and assess the fine scale consequences of abatement measures.

Author contributions

The manuscript was written through contributions of all authors. All authors have given approval to the final version of the manuscript. All authors contributed equally.

Acknowledgments

This work was supported by NSF SCOPE project grant #IIP1430145 and NASA Carbon Monitoring System grant #NNH13CK02C. ISW gratefully acknowledges support from NSF (grant #GEO-1240507). The authors would also like to thank the Central Transportation Planning Staff of the Boston MPO, and Steven C. Wofsy of Harvard University for their assistance.

Appendix A. Supplementary data

Supplementary data related to this article can be found at http://dx.doi.org/10.1016/j.envpol.2017.05.091.

References

Anderson, D.C., Loughner, C.P., Diskin, G., Weinheimer, A., Canty, T.P., Salawitch, R.J., Worden, H.M., Fried, A., Mikoviny, T., Wisthaler, A., et al., 2014. Measured and modeled CO and NOy in DISCOVER-AQ: an evaluation of emissions and chemistry over the eastern US. Atmos. Environ. 96, 78–87.

Barth, M., Boriboonsomsin, K., 2008. Real-world carbon dioxide impacts of traffic congestion. Transp. Res. Rec. J. Transp. Res. Board 2058, 163–171.

Boston Metropolitan Planning Organization, 2017. Central transportation planning Staff, TransCAD travel demand model. Details available at. http://www.ctps.org/data/html/studies/other/Travel_Modeling_101.htm (Accessed 1 January 2017).

Cervero, R., Kockelman, K., 1997. Travel demand and the 3Ds: density, diversity, and design. Transp. Res. Part D. Transp. Environ. 2 (3), 199–219.

Choi, D., Beardsley, M., Brzezinski, D., Koupal, J., Warila, J., 2010. MOVES sensitivity Analysis : the impacts of temperature and humidity on emissions. 19th Int. Emiss. Invent. Conf. San. Ant. Tex. S6, P1.

Dallmann, T.R., Harley, R.A., 2010. Evaluation of mobile source emission trends in the United States. J. Geophys. Res. 115 (D14), D14305.

Dowling, R., Skabardonis, A., 1993. Improving the average travel speeds estimated by planning models. Transp. Res. Rec. 1360, 68–74.

Dowling, R., 1997. Planning Techniques to Estimate Speeds and Service Volumes for Planning. National Cooperative Highway Research planning report 387. National Research Council, Washington, DC.

Ewing, R., Cervero, R., 2001. Travel and the built environment: a synthesis. Transp. Res. Rec. 1780 (1), 87–114.

Federal Highway Administration, 2012a. Highway statistics series, table HM-71. Washington, DC. http://www.fhwa.dot.gov/policyinformation/statistics (Accessed 1 July 2016).

Federal Highway Administration, 2012b. Highway statistics series, table MF-21. Washington, DC. http://www.fhwa.dot.gov/policyinformation/statistics (Accessed 1 July 2016).

Gately, C.K., Hutyra, L.R., Sue Wing, I., 2015. Cities, traffic, and CO_2: a multidecadal assessment of trends, drivers, and scaling relationships. Proc. Natl. Acad. Sci. U. S. A. 112 (16), 4999–5004.

Gurney, K.R., Romero-Lankao, P., Seto, K.C., Hutyra, L.R., Duren, R.M., Kennedy, C., Grimm, N.B., Ehleringer, J.R., Marcotullio, P., Hughes, S., et al., 2015. Track urban emissions on a human scale. Nature 525 (7568), 179–181.S.

Harley, R.A., McKeen, S.A., Pearson, J., Rodgers, M.O., Lonneman, W.A., 2001. Analysis of motor vehicle emissions during the Nashville/Middle Tennessee ozone study. J. Geophys. Res. 106 (D4), 3559–3567.

Huang, C., Chen, C.H., Li, L., Cheng, Z., Wang, H.L., Huang, H.Y., Streets, D.G., Wang, Y.J., Zhang, G.F., Chen, Y.R., 2011. Emission inventory of anthropogenic air pollutants and VOC species in the yangtze river delta region, China. Atmos. Chem. Phys. 11 (9), 4105–4120.

Hutyra, L.R., Duren, R., Gurney, K.R., Grimm, N., Kort, E. a., Larson, E., Shrestha, G., 2014. Urbanization and the carbon cycle: current capabilities and research outlook from the natural sciences perspective. Earth's Future. 2 (10), 2014EF000255.

Hymel, K.M., Small, K.A., Van Dender, K., 2010. Induced demand and rebound effects in road transport. Transp. Res. Part B Methodol. 44 (10), 1220–1241.

Jacob, D.J., Winner, D.A., 2009. Effect of climate change on air quality. Atmos. Environ. 43 (1), 51–63.

Kim, S.W., McDonald, B.C., Baidar, S., Brown, S.S., Dube, B., Ferrare, R.A., Frost, G.J., Harley, R.A., Holloway, J.S., Lee, H.J., et al., 2016. Modeling the weekly cycle of NOx and CO emissions and their impacts on O3 in the Los angeles-south coast air basin during the CalNex 2010 field campaign. J. Geophys. Res. Atmos. 121 (3), 1340–1360.

Kinney, P.L., 2008. Climate change, air quality, and human health. Am. J. Prev. Med. 35 (5), 459–467.

Koupal, J., DeFries, T., Palacios, C., Fincher, S., Preusse, D., 2014. Motor vehicle emissions simulator input data. Transp. Res. Rec. J. Transp. Res. Board 2427, 63–72.

Lauvaux, T., Schuh, a. E., Bocquet, M., Wu, L., Richardson, S., Miles, N., Davis, K.J., 2012. Network design for mesoscale inversions of CO2 sources and sinks. Tellus B 64, 17980.

Lazaridis, M., Aleksandropoulou, V., Aleksandropoulou, V., Hanssen, J., Dye, C., Dye, C., Eleftheriadis, K., Katsivela, E., Martello, D., Pekney, N., et al., 2008. Resolving local-scale emissions for modeling air quality near roadways. J. Air Waste Manage. Assoc. 58 (3), 451–461.

Lelieveld, J., Evans, J.S., Fnais, M., Giannadaki, D., Pozzer, A., 2015. The contribution of outdoor air pollution sources to premature mortality on a global scale. Nature 525 (7569), 367–371.

Massachusetts Department of Transportation, 2012. Massachusetts Travel Survey, 2012 Final Report, Appendices. Prepared for the Massachusetts Department of Transportation by Nustats Research Solutions, Austin, TX. http://www.mass.gov/massdot/travelsurvey.

McDonald, B.C., Dallmann, T.R., Martin, E.W., Harley, R.A., 2012. Long-term trends in nitrogen oxide emissions from motor vehicles at national, state, and air basin scales. J. Geophys. Res. Atmos. 117, D00V18. http://dx.doi.org/10.1029/2012JD018304.

McDonald, B., McBride, Z., Martin, E.W., Harley, R. a, 2014. High-resolution mapping of motor vehicle carbon dioxide emissions. J. Geophys. Res. Atmos. 119 (May), 5283–5298.

NCAR community. June 2004. Community climate system model, version 3.0. http://www.cesm.ucar.edu/models/ccsm3.0/NCAR/UCAR. GIS data services are provided by NCAR GIS Program through Climate Change Scenarios, version 2.0, 2012; http://www.gisclimatechange.org (Accessed 1 November 2015).

Noland, R.B., 2000. Relationships between highway capacity and induced vehicle travel. Transp. Res. Part A Policy Pract. 35 (1), 47–72.

Nyhan, M., Sobolevsky, S., Kang, C., Robinson, P., Corti, A., Szell, M., Streets, D., Lu, Z., Britter, R., Barrett, S.R.H., et al., 2016. Predicting vehicular emissions in high spatial resolution using pervasively measured transportation data and microscopic emissions model. Atmos. Environ. 140, 352–363.

Olivier, J., van Aardenne, J.A., Dentener, F., Ganzeveld, L., Peters, J.A.H.W., 2005. Recent trends in global greenhouse gas emissions: regional trends 1970-2000 and spatial distribution of key sources in 2000. J. Integr. Env. Sci. 2 http://dx.doi.org/10.1080/15693430500400345.

Parrish, D.D., 2006. Critical evaluation of US on-road vehicle emission inventories. Atmos. Environ. 40 (13), 2288–2300.

Schifter, I., Díaz, L., Múgica, V., López-Salinas, E., 2005. Fuel-based motor vehicle emission inventory for the metropolitan area of Mexico city. Atmos. Environ. 39 (5), 931–940.

Schrank, D., Lomax, T., Eiselle, B., 2012. The 2012 Urban Mobility Report. Texas Transportation Institute, Texas A&M University, College Station, TX. http://mobility.tamu.edu/ums/ (Accessed 1 May 2015).

Skabardonis, A., Dowling, R., 1997. Improved speed-flow relationships for planning

applications. Transp. Res. Rec. 1572, 18–23.
Small, K. a., Van Dender, K., 2007. Fuel efficiency and motor vehicle travel: the declining rebound effect. Energy J. 28 (1), 25–51.
Snyder, M., Arunachalam, S., Isakov, V., Talgo, K., Naess, B., Valencia, A., Omary, M., Davis, N., Cook, R., Hanna, A., 2014. Creating locally-resolved mobile-source emissions inputs for air quality modeling in support of an exposure study in detroit, Michigan, USA. Int. J. Environ. Res. Public Health 11 (12), 12739–12766.
Steiner, A.L., Tonse, S., Cohen, R.C., Goldstein, A.H., Harley, R.A., 2006. Influence of future climate and emissions on regional air quality in California. J. Geophys. Res. 111 (D18), D18303.
Streets, D.G., Canty, T., Carmichael, G.R., de Foy, B., Dickerson, R.R., Duncan, B.N., Edwards, D.P., Haynes, J.A., Henze, D.K., Houyoux, M.R., Jacobi, D.J., Krotkov, N.A., Lamsal, L.N., Liu, Y., Lu, Z.F., Martini, R.V., Pfister, G.G., Pinder, R.W., Salawitch, R.J., Wechti, K.J., 2013. Emissions estimation from satellite retrievals: a review of current capability. Atmos. Environ. 77, 10111042. http://dx.doi.org/10.1016/j.atmosenv.2013.05.051.
U.S. Environmental Protection Agency, 2011a. National multipollutant emissions comparison by source sector. U.S. Environmental Protection Agency, Washington, DC. http://www.epa.gov/air/emissions/multi.htm (Accessed 1 January 2016).
U.S. Environmental Protection Agency, 2011b. State and county emissions summaries. U.S. Environmental Protection Agency, Washington, DC. http://www.epa.gov/air/emissions/where.htm (Accessed 1 January 2016).
U.S. Environmental Protection Agency, 2011c. National emissions inventory 2011. Washington, DC. https://www.epa.gov/air-emissions-inventories/2011-national-emissions-inventory-nei-data (Accessed 1 July 2016).
U.S. Environmental Protection Agency, 2014a. Near roadway pollution and health. U.S. Environmental Protection Agency, Washington, DC. http://www.epa.gov/otaq/documents/nearroadway/420f14044.pdf (Accessed 1 June 2016).
U.S. Environmental Protection Agency, 2014b. Motor vehicle emission simulator (MOVES 2014). U.S. Environmental Protection Agency, Washington, DC. http://www.epa.gov/otaq/models/moves/index.htm (Accessed 1 December 2015).
U.S. Environmental Protection Agency, 2015a. Exhaust Emission Rates for Light-duty On-road Vehicles in MOVES2014. Report No. EPA-420-R-15-005, October 2015. U.S. Environmental Protection Agency, Washington, DC.
U.S. Environmental Protection Agency, 2015b. Emission Adjustments for Temperature, Humidity, Air Conditioning, and Inspection and Maintenance for On-road Vehicles in MOVES2014. EPA-420-R-15-020, November 2015. U.S. Environmental Protection Agency, Washington, DC.
Wang, C., Prinn, R.G., 1999. Impact of emissions, chemistry and climate on atmospheric carbon monoxide: 100-yr predictions from a global chemistry–climate model. Chemosph. - Glob. Chang. Sci. 1 (1–3), 73–81.
West, B.H., McGill, R.N., Hodgson, J.W., Sluder, S.S., Smith, D.E., 1999. Development and Validation of Light-duty Vehicle Modal Emissions and Fuel Consumption Values for Traffic Models, Report No. FHWA-rd-00–068. Federal Highway Administration, Washington, DC.
Wu, L., Bocquet, M., Lauvaux, T., Chevallier, F., Rayner, P., Davis, K., 2011. Optimal representation of source-sink fluxes for mesoscale carbon dioxide inversion with synthetic data. J. Geophys. Res. Atmos. 116 (21), 1–16.
Xia, Y., Mitchell, K., Ek, M., Sheffield, J., Cosgrove, B., Wood, E., Luo, L., Alonge, C., Wei, H., Meng, J., et al., 2012. Continental-scale water and energy flux analysis and validation for the North american land data assimilation system project phase 2 (NLDAS-2): 1. Intercomparison and application of model products. J. Geophys. Res. 117 (D3), D03109.
Xing, J., Pleim, J., Mathur, R., Pouliot, G., Hogrefe, C., Gan, C.M., Wei, C., 2013. Historical gaseous and primary aerosol emissions in the United States from 1990 to 2010. Atmos. Chem. Phys. 13 (15), 7531–7549.
Zhang, K., Batterman, S., Dion, F., 2011. Vehicle emissions in congestion: comparison of work zone, rush hour and free-flow conditions. Atmos. Environ. 45 (11), 1929–1939.
Zheng, J., Zhang, L., Che, W., Zheng, Z., Yin, S., 2009. A highly resolved temporal and spatial air pollutant emission inventory for the pearl river delta region, China and its uncertainty assessment. Atmos. Environ. 43 (32), 5112–5122.
Zhou, Y., Levy, J.I., 2007. Factors influencing the spatial extent of mobile source air pollution impacts: a meta-analysis. BMC Public Health 7, 89.
Zhu, Y., Hinds, W.C., Kim, S., Sioutas, C., 2002. Concentration and size distribution of ultrafine particles near a major highway. J. Air Waste Manag. Assoc. 52 (9), 1032–1042.
Zwack, L.M., Paciorek, C.J., Spengler, J.D., Levy, J.I., 2011a. Modeling spatial patterns of traffic-related air pollutants in complex urban terrain. Environ. Health Perspect. 119 (6), 852–859.
Zwack, L.M., Paciorek, C.J., Spengler, J.D., Levy, J.I., 2011b. Characterizing local traffic contributions to particulate air pollution in street canyons using mobile monitoring techniques. Atmos. Environ. 45 (15), 2507–2514.

SUPPLEMENTARY INFORMATION

Details of Data Sources

INRIX Traffic Speeds

The INRIX database of average hourly vehicle speed by segment is derived from thousands of mobile phone and vehicle GPS devices, which are then aggregated by INRIX to calculate average travel speed on over 60,000 road segments in our study domain at 5-minute intervals for the year 2012. The INRIX road network separates vehicle travel on each road segment by the direction of travel, to account for the variation in daily traffic patterns on roads that experience distinct directional patterns of traffic activity depending on the time of day. The georeferenced Massachusetts Road Inventory (MRI) road network forms the spatial basis for our emissions model, but lacks a crosswalk to unique road segment IDs in the INRIX database. We therefore merged the two datasets in a GIS using a proximity-based spatial join. Manual validation of road segments in the merged dataset was undertaken by Boston MPO CTPS staff for major roadways. This procedure was completed for all road segments by the authors.

Traffic Volumes

The MRI shapefile contains estimates of ADT volumes for each road segment, as well as the number of lanes in the segment and the roadway functional class as defined by FHWA. ADT estimates were missing for some road segments, mostly local roads. However, estimates of total vehicle-miles travelled on local roads in the Boston Urbanized Area are available from the FHWA Highway Statistics Series Table HM-71 (FHWA 1980-2012). We used these aggregate totals to assign an average ADT to each Boston Urbanized Area local road with missing observations in the MRI. The procedure is as follows. We first subtracted total VMT from the local roads that do have a reported ADT from the total VMT in Table HM-71, and then divide the remaining VMT by the total length of all the local roads that are missing VMT in the Urbanized Area, and then divide again by 366 days, to get an average daily traffic volume for all local roads.

CTPS Highway Assignment Model

We joined output from the CTPS highway assignment travel demand model (TDM) year 2012 base run to the MRI attribute table. The highway assignment model is implemented using the TransCAD traffic modeling software, and is continuously updated and maintained by CTPS as part of its mission to model and forecast local and regional transportation system demand. The model output we use is the final component of a larger model set which follows the well-known four-step transportation modeling procedure:

1. Trip generation: estimation of the number of daily trips in Eastern Massachusetts, based on travel survey data, vehicle fleet data, and demographic information. Freight trips are estimated separately from non-freight trips. Trip generation is estimated for four time periods: AM peak (6am – 10am), Midday (10am – 3pm), PM peak (3pm – 7pm), and Nighttime (7pm – 6am).
2. Trip distribution: using the same data on land-use and travel patterns, the location of trip origins and destinations is estimated and aggregated to traffic analysis zones (TAZs). Freight trips are again assigned separately from non-freight trips. Data output from the distribution step are matrices of the freight and non-freight trips by origin-destination (O-D) pairs for all TAZs in the domain.
3. Mode choice: assignment of trips in the O-D matrices created in step 2 to different travel modes. Non-freight trips are divided amongst passenger cars, SUVs and pickups, public transit (buses and light and heavy rail), bicycling, and walking. Freight trips are divided amongst large and medium class trucks (i.e. combination tractor trailer and single-unit trucks, respectively).

4. Route assignment: allocation of trips to individual segments of the relevant transportation network (roads, heavy/light rail, cycling infrastructure, etc.) using optimization techniques to minimize total travel delay while satisfying constraints of origin-destination travel demands and link capacities. Additional details of the CTPS model are available at: http://www.ctps.org/data/html/studies/other/Travel_Modeling_101.htm

We utilize the TDM model output consisting of estimated vehicle travel for four representative periods of a weekday (τ): AM peak (6am-10am), mid-day (10am-3pm), PM peak (3pm-7pm), and night (7pm-6am), stratified by vehicle type and road segment direction. The model also provides information on key characteristics of each segment: its capacity (K) and the coefficients (α and β) of its link-performance function, which follows a modified Bureau of Public Roads volume-delay formulation with free flow speed S^{FF}:

$$\overline{S}_{l,\tau} = S_l^{FF}\left(1 + \alpha_l \cdot v_{l,\tau}/K_l\right)^{-\beta_l} \qquad \textit{(Eqn. S1)}$$

For roads without records in the INRIX database, the above equation was used to impute vehicle speeds ($\overline{S}_{l,\tau}$). CTPS has developed customized coefficients (α and β) for *Eqn. S1* that vary according to road functional class and location within the urban area. These coefficients have been calibrated against traffic counts and 'floating car' data on vehicle speeds at multiple locations across the region. Generally, the values for α range from 0.8 to 1.25, and the values for β range from 4 to 5.5.

Simulated traffic volumes are not used directly, as the output of the model does not cover all MRI road segments, and many local roads are excluded to keep the assignment problem computationally tractable. For consistency, MRI AADT for each link is taken as the control total, and CTPS model output used to disaggregate this volume by time of day, travel direction, and vehicle type. Vehicle types are stratified into five aggregate classes: passenger cars (gasoline powered), passenger trucks (SUVs and pickups, both gasoline powered), medium-size trucks (gasoline-powered), medium-size trucks (diesel-powered), and heavy trucks (diesel-powered). We aggregate buses into the "heavy truck" vehicle class. Modeled volumes by vehicle class in each of the four time periods were divided by the modeled total daily link volume (by direction), generating a vector of shares by vehicle class, direction, and time of day that were then used to split MRI AADT. MRI road segments missing from the CTPS model were assigned the characteristics of the nearest modeled road segment belonging to the same functional class.

Hourly Time Structure

To temporally disaggregate MRI AADT we use a large dataset of hourly traffic counts from 62 permanent traffic recorders (PTRs) across the study region (Massachusetts Department of Transportation 2014). Counts are obtained from inductive loop sensors embedded in the roadway surface that continuously monitor traffic throughout the year. For each PTR station we divide the vehicle counts at each hour by total annual count for the year 2012 to calculate an hourly share. We assign each MRI roadway link the hourly traffic profile of the closest PTR. Road segments' hourly traffic volumes are then estimated by multiplying AADT by 366 days and the hourly share.

Speed Assignment

All MRI links matching INRIX road segments were assigned the INRIX mean hourly speed for each hour of the year. Computational tractability necessitated aggregation of the raw 5-min INRIX speeds to an hourly time step. For a link belonging to a particular roadway functional class, free-flow speed was imputed as the mean of the 85th percentile of speeds calculated for all roads in that functional class in the INRIX database. The resulting values of S^{FF} were assigned to MRI segments missing observations in the INRIX database.

Emission Factors

Emissions factors were calculated using the latest version of EPA's Motor Vehicle Emissions Simulator (MOVES2014). MOVES contains default values for many of the parameters used to determine emission rates. EPA strongly recommends that users include as much local data as possible when running the model, so as to minimize biases due to mismatch between the parameter defaults and actual local parameter values. MOVES' spatial resolution is limited to the county scale in "inventory" mode, but finer resolution estimates of emissions can be calculated in "emission factor" mode, which produces an output table of grams of pollutant emissions per vehicle kilometer travelled (VKT) for a range of vehicles and fuel types. We generate emissions factors for CO_2 as well as four other air pollutants (CO, NO_2, NO_x, and $PM_{2.5}$).

Emissions factors are highly sensitive to the specification of atmospheric conditions, vehicle make, model, age and fuel, and to the speed of travel, with MOVES requiring inputs characterizing all of these variables for the study domain (Figures S4,S5). CTPS, in the course of modeling and forecasting the air quality impacts of regional transportation, has developed a set of dedicated input parameters specific to Eastern Massachusetts. We use data on the vehicle fleet composition (vehicle type and age) for Middlesex County, MA derived by CTPS from vehicle registration data obtained from the State Registry of Motor Vehicles. CTPS also provided us with data on the fuel formulation for motor fuels sold in Middlesex County, MA. We augment these custom inputs with a table that covers the full range of meteorological conditions in the year 2012, obtained from NLDAS-2 reanalysis at 0.125° resolution of gridded hourly surface temperatures at 2 meter elevation and specific humidity.

Meteorological Impacts on Emissions

Meteorological variables required by MOVES are ambient atmospheric temperature and relative humidity. NLDAS-2 reports hourly 2m air temperature, pressure, and specific humidity, from which we generated hourly relative humidity using the Clausius-Clapeyron equation. Each grid cell's hourly temperature and relative humidity were assigned to its constituent road segments.

We performed MOVES runs to generate emission factors for our target pollutants for every combination of temperature in 1C intervals, relative humidity in 10 percentage-point intervals, vehicle speed in 5 mph bins, our 5 aggregated vehicle types, and road functional class. The resulting matrix of factors was merged with our hourly vehicle activity data by assigning every vehicle type's specific emissions to road links on the basis of hourly temperature, relative humidity, and speed. The final output consists of hourly estimates of emissions of the five pollutants of interest for each of the five vehicle types, for each of the ~280,000 road segments in the domain.

Supplemental Figures

Figure S1 shows the methods for integrating the above data streams to produce hourly emissions estimates at road-segment scale. Figure S2 shows the comparison of CO_2 running emissions from this study with estimates from the DARTE inventory product for the year 2012. Figure S3 shows the estimated changes in annual emissions of CO in 2050 resulting from higher mean monthly temperatures forecast to occur under the IPCC Representative Concentration Pathway 8.5. Figures S4 and S5 show the variation in MOVES emissions factors for NO_x and $PM_{2.5}$ as a function of temperature, vehicle speed, and vehicle type.

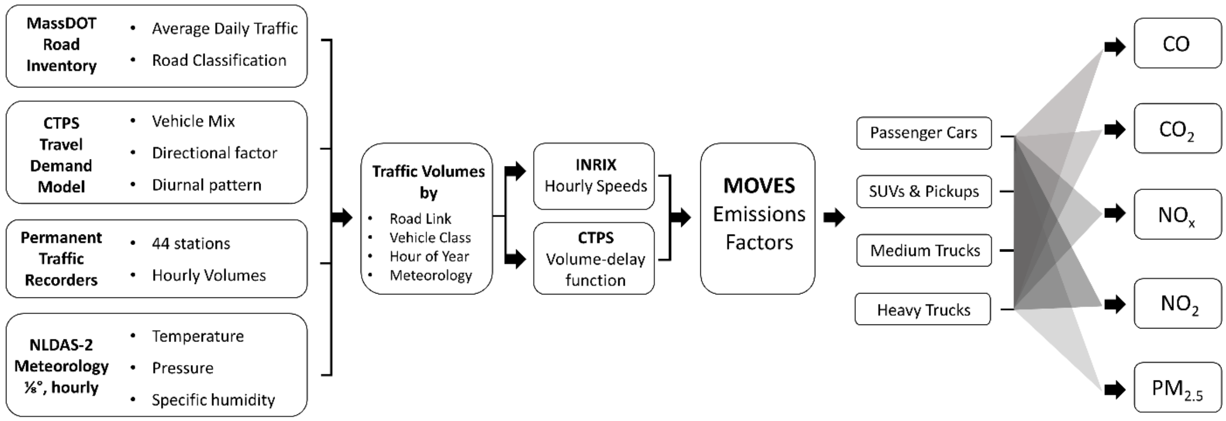

Figure S1. Data fusion methodology. The four major input datasets are spatially merged to generate hourly traffic volumes for 5 vehicle types for each of the 280,424 road segments in the domain, coupled to the hourly ambient meteorology for each road. Traffic flow speeds are assigned to segments using INRIX data (where available), or else imputed using *Eqn. S1*. Emission factors for CO, CO_2, NO_2, NO_x, and $PM_{2.5}$ are calculated using MOVES2014 for all combinations of vehicle types, speed intervals, and temperature and humidity regimes, and then applied to the hourly traffic volumes of each vehicle class accordingly.

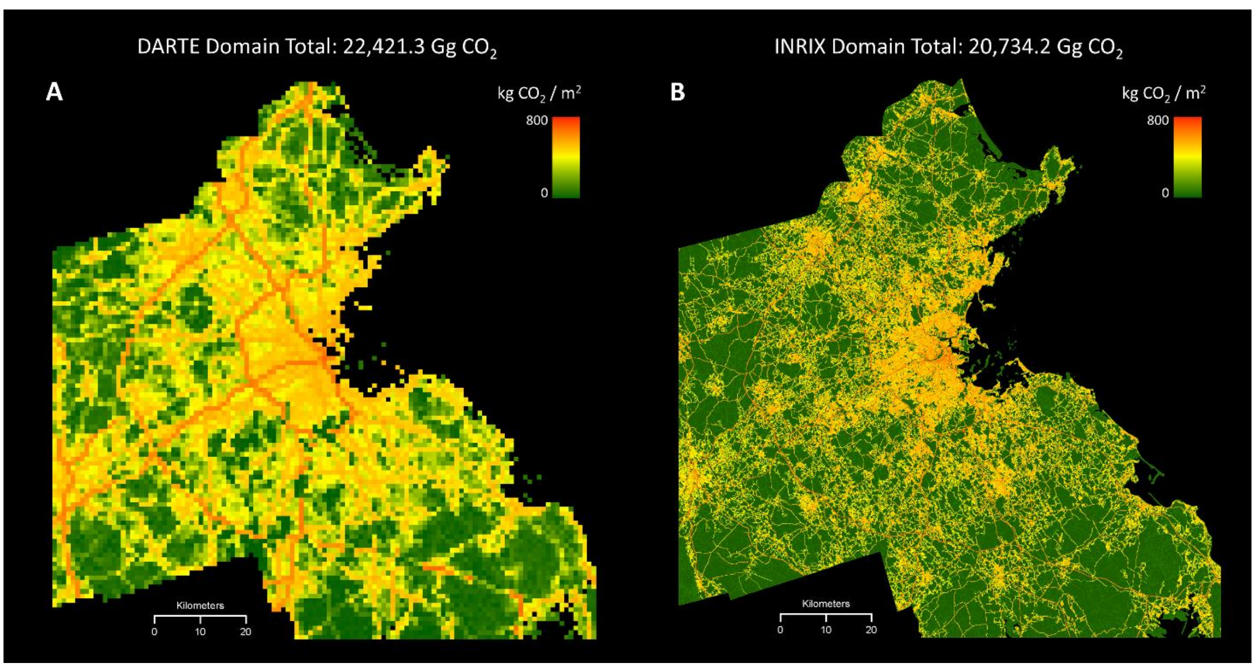

Figure S2. Comparison of on-road CO_2 running emissions between DARTE (A) and our INRIX-based model (B) for the year 2012. The spatial resolution of DARTE (left panel) is 1km x 1km. The spatial resolution of the INRIX-based model is 100m x 100m. The total estimates for annual CO_2 emissions are within 8%, suggesting that DARTE captures the overall intensity of on-road emissions well, despite not directly accounting for variations in vehicle speeds or local meteorology.

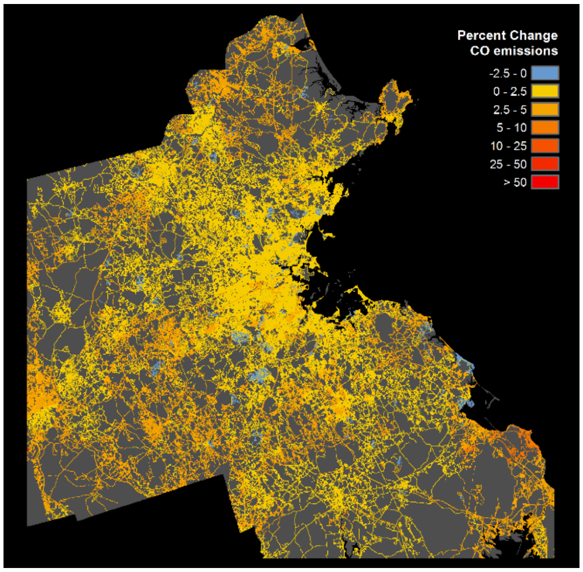

Figure S3. Annual change in CO emissions in 2050 resulting from increases in mean ambient temperature. Increases of 2.5 – 5% are estimated to occur broadly over the study area. Larger increases of 10 – 25 % or more are predicted in many localized areas. Small areas may experience modest decreases in CO emissions of ~1-2%.

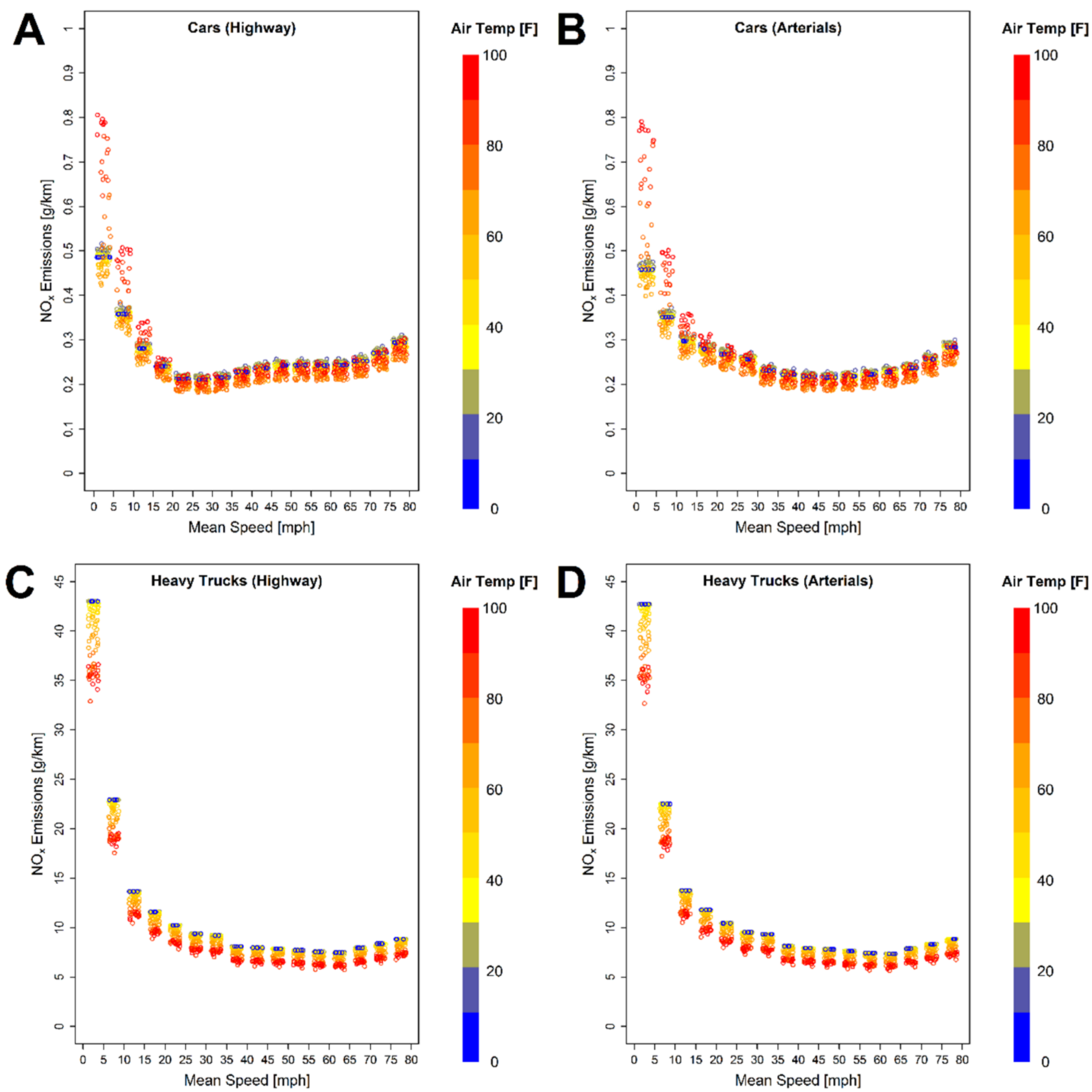

Figure S4. Comparison of MOVES2014 emissions factors for NOx from passenger cars and heavy trucks as a function of road type, speed and temperature. NO_x emission rates are highest at low vehicle speeds for all vehicle types and road types. However, at low speeds emission rates show opposite trends with temperature for gasoline-powered passenger cars and diesel-powered heavy trucks. At high temperatures and low speeds, NOx emissions rates are significantly enhanced for passenger cars, while for heavy trucks colder temperatures at low speeds are associated with the highest emissions factors.

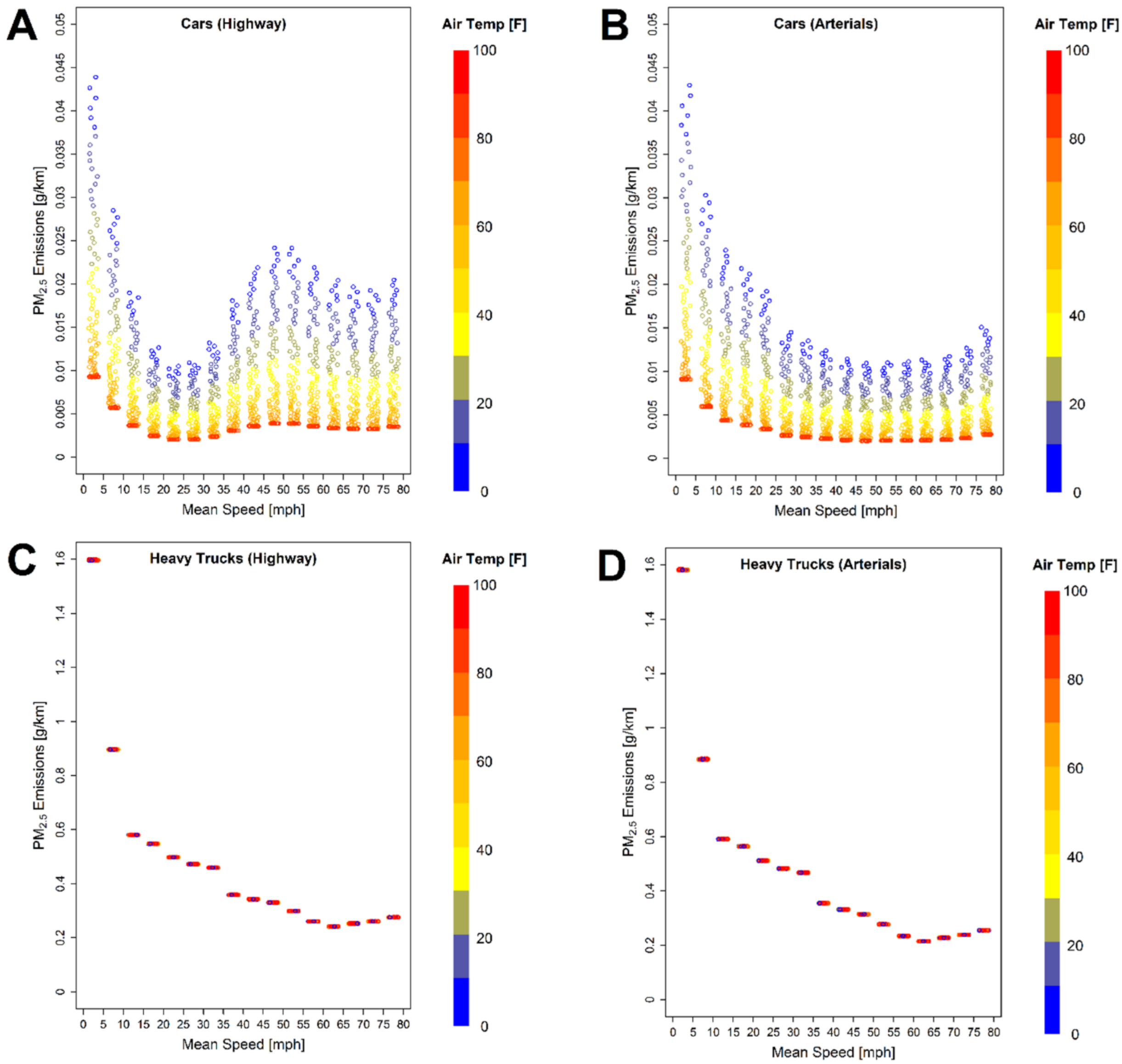

Figure S5. Comparison of MOVES2014 emissions factors for $PM_{2.5}$ from passenger cars and heavy trucks as a function of road type, speed, and temperature. MOVES currently does not vary the emissions factors for heavy truck $PM_{2.5}$ with temperature. For passenger cars, cold temperatures have a significant positive effect on emissions across all vehicle speeds, with the largest effect at low speeds. The effect of low speeds on heavy truck $PM_{2.5}$ is also significant, with large increases seen at speeds below 35 mph. For cars, the impact of lower speeds on emissions is most visible on Arterial roads, due to the drive-cycle characteristics MOVES uses for these roads.